OPEN

PRS GLOBAL OPEN

ORIGINAL ARTICLE
Research

An Inexpensive 3D Printed Mouse Model of Successful, Complication-free Long Bone Distraction Osteogenesis

Ruth Tevlin, MB, BAO, BCh, MRCSI, MD*†‡
Harsh N. Shah, MPH, MS†
Ankit Salhotra, BS†§
Sarah E. Di Iorio, SB†¶
Michelle Griffin, MBChB, MRCS, PhD†
Michael Januszyk, MD, PhD†
Derrick C. Wan, MD*†
Michael T. Longaker, MD, MBA, FACS*†§¶

Background: Distraction osteogenesis (DO) is used for skeletal defects; however, up to 50% of cases exhibit complications. Previous mouse models of long bone DO have been anecdotally hampered by postoperative complications, expense, and availability. To improve clinical techniques, cost-effective, reliable animal models are needed. Our focus was to develop a new mouse tibial distractor, hypothesized to result in successful, complication-free DO.

Methods: A lightweight tibial distractor was developed using CAD and 3D printing. The device was fixed to the tibia of C57Bl/6J mice prior to osteotomy. Postoperatively, mice underwent 5 days latency, 10 days distraction (0.15 mm every 12 hours), and 28 days consolidation. Bone regeneration was examined on postoperative day 43 using micro-computed tomography (μCT) and Movat's modified pentachrome staining on histology (mineralized volume fraction and pixels, respectively). Costs were recorded. We compared cohorts of 11 mice undergoing sham, DO, or acute lengthening (distractor acutely lengthened 3.0 mm).

Results: The histological bone regenerate was significantly increased in DO (1,879,257±155,415 pixels) compared to acute lengthening (32847±1589 pixels) ($P < 0.0001$). The mineralized volume fraction (bone/total tissue volume) of the regenerate was significantly increased in DO (0.9±0.1) compared to acute lengthening (0.7±0.1) ($P < 0.001$). There was no significant difference in bone regenerate between DO and sham. The distractor was relatively low cost ($11), with no complications.

Conclusions: Histology and μCT analysis confirmed that the proposed tibial DO model resulted in successful bone formation. Our model is cost-effective and reproducible, enabling implementation in genetically dissectible transgenic mice.
(Plast Reconstr Surg Glob Open 2023; 11:e4674; doi: 10.1097/GOX.0000000000004674; Published online 13 February 2023.)

*From the *Division of Plastic and Reconstructive Surgery, Stanford University School of Medicine, Stanford, Calif.; †Hagey Laboratory for Pediatric Regenerative Medicine, Department of Surgery, Stanford University School of Medicine, Stanford, Calif.; ‡Department of Bioengineering and Regenerative Medicine, Royal College of Surgeons in Ireland, St. Stephen's Green, Dublin, Ireland; §Institute for Stem Cell Biology and Regenerative Medicine, Stanford University School of Medicine, Stanford, Calif.; and ¶Stanford University School of Medicine, Stanford, Calif.*

Received for publication September 8, 2022; accepted September 27, 2022.

Drs. Tevlin, Shah, and Salhotra contributed equally to this work.

Presented at the American College of Surgeon Clinical Congress 2020, International Society for Stem Cell Research 2020 Annual Meeting, Wound Healing Society 2020 Annual Meeting, and Plastic Surgery Research Council Annual Meeting 2020.

DOI: 10.1097/GOX.0000000000004674

INTRODUCTION

Segmental long bone defects arise from a myriad of pathologies including high-velocity trauma, surgical

Funding: This work was supported by the Oak Foundation and the Hagey Laboratory for Pediatric Regenerative Medicine. R. T. was supported by the Plastic Surgery Research Council Research Fellowship Grant, the Stanford University Tissue Engineering and Center of Excellence Research Grant, and the American Society of Maxillofacial Surgery Research Grant. M. G. was supported by the Stanford University Tissue Engineering and Center of Excellence Research Grant. M. T. L. was supported by NIH Grant R01 DE026730 and R01 DE027323. H. N. S. was supported by NIH Grant 5T32GM119995-02. S. E. D. I. was supported by the Stanford University Medical Scientist Training Program grant T32-GM007365. Micro-CT was performed using equipment supplied by NIH S10 grant 1S10OD02349701, PI: Timothy C. Doyle.

Disclosure: *The authors have no financial interest to declare in relation to the content of this article.*

resection of tumors, osteomyelitis, and fracture malunion. A critical-sized bone defect is regarded as one that will not heal spontaneously despite surgical stabilization and, thus, requires further intervention to "fill" the bony gap.[1] Management of critical-sized bone defects continues to represent a major clinical challenge. Options, such as bone allograft and autograft, are fraught with limitations.[2,3] Distraction osteogenesis (DO) is an alternative limb-preserving treatment, first described in humans by Codivilla in 1905[4] and which later gained notoriety following work by Ilizarov in World War II.[4,5] DO is divided into three key steps: a latency period for callus development, a distraction period of gradual lengthening, and a consolidation period that allows the regenerate to mineralize.[5–7] While DO results in endogenous bone formation, the procedure is not without its own unique challenges. The process is lengthy, spanning approximately 1 year.[5] Furthermore, two case series and a meta-analysis support that there is up to a 50% complication rate, including malunion, delayed union, or failure.[5,8,9] Additional research is needed to optimize this technique and reduce complications.

The majority of animal studies to date regarding long bone DO have been performed in rabbits,[10–12] micropigs,[13–15] dogs,[16,17] and rats[18–24]; however, these experimental methods are limited given the paucity of transgenic animals for interrogation and the expense of these experimental models. Several techniques of mouse tibial DO have been proposed, which implement specialist dental equipment or human devices adapted to a mouse model; however, these methods have been hampered by postoperative complications and negative effect on mouse mobility, as reported in the use of circular frames.[25,26] In addition, to date, results of studies pertaining to mice have not translated into clinical advances.[27–29] Another current gap in research is the expense and availability of existing models.[25,26,30] While exact costs of other DO models are not directly reported, the use of materials, such as immediate polymerization resin,[25] specialized metal distractors adapted from craniofacial DO,[30] and aluminum and stainless steel distractor components,[26] demonstrates the lack of an existing low-cost small animal distractor. A low-cost and easily accessible mouse long bone DO model has the ability to accelerate animal research, as the mouse models are genetically dissectible (eg, availability of transgenic animals). Small animal research could then translate to large animal models, and ultimately from the bench to the bedside, thus offering promise of improvement in clinical outcomes for our patients undergoing long bone DO.

The purpose of this study was to establish a new method of tibial DO in mice, which utilizes a computer-aided design of a lightweight fixator in addition to commercially available screws. Our new model used inexpensive and more easily manufactured materials relative to current models and a monolateral rather than circular frame. We hypothesized that this new model of tibial DO would be low cost and lead to robust, complication-free osteogenesis, which could be validated both radiologically and histologically at the end of the consolidation phase in comparison with sham and acutely lengthened bones.

Takeaways

Question: Distraction osteogenesis (DO) results in bone regeneration but is associated with prolonged treatment and complications such as malunion and failure. The aim of this study was to develop a rigorously tested, reproducible and cost-effective long bone DO mouse model.

Findings: We demonstrate the use of a method of long bone DO, which utilizes a computer-aided design of a lightweight monolateral fixator in addition to commercially available screws.

Meaning: This model of mouse tibial DO results in reproducible and reliable osteogenesis and holds great promise to accelerate research and improve clinical outcomes for patients undergoing long bone DO.

METHODS

Animals

Ten-week-old male mice, C57BL/6J mice, (Jackson Laboratories) were used for development and testing of the surgical model. Mice were divided into three groups: sham, acute lengthening, and a gradually distracted group. All mice were killed on postoperative day (POD) 43, mirroring our laboratory's mandibular distraction protocol[31] and previously published models.[32,33] All experiments were performed according to Stanford University Animal Care and Use Committee guidelines. Animals were housed in cages of up to five littermates in temperature- and light-controlled environments and fed *ad libitum*.

Development of the Tibial Distractor

The tibial distraction devices were manufactured using computer-aided design as previously described.[31] Briefly, the computer-aided designed distractors were 3D printed using a light-weight UV-cured photopolymer composed of urethane acrylate oligomers (20%–40%), ethoxylated bisphenol A diacrylate (15%–35%), and tripropyleneglycol diacrylate (1.5%–3%) (Fig. 1). As evident in Figure 1, there were two distractor footplates printed in each 3D printing run, and these were then divided (cut with scissors) before placement on the tibia. The screws used were purchased from a commercial supplier (Mc Master Carr, Ohio.). For the distractor plate fixation to the tibia, 18-8 Stainless Steel Pan Head Torx Screws (000-120 thread size, 1/8" length, 96710A001) were used. For the distractor screw, a Super-Corrosion-Resistant 316 Stainless Steel Socket Head Screw (0-80 thread size, ½ inch length, 92185A055) was used. A dental drill (Brasseler Z500, Ga.) was used both for screw fixation (0.6-mm drill bit, Drill Bit City, Illi.) to the tibia and for osteotomy (0.2 mm, Medium MiniFlex Double Sided Diamond Disc, Brasseler Dental Instrumentation, Ga.). The cost of distractor parts was recorded.

Tibial Distractor Placement

In accordance with Stanford University Animal Care and Use Committee guidelines, mice were placed under multimodal anesthesia composed of intraperitoneal

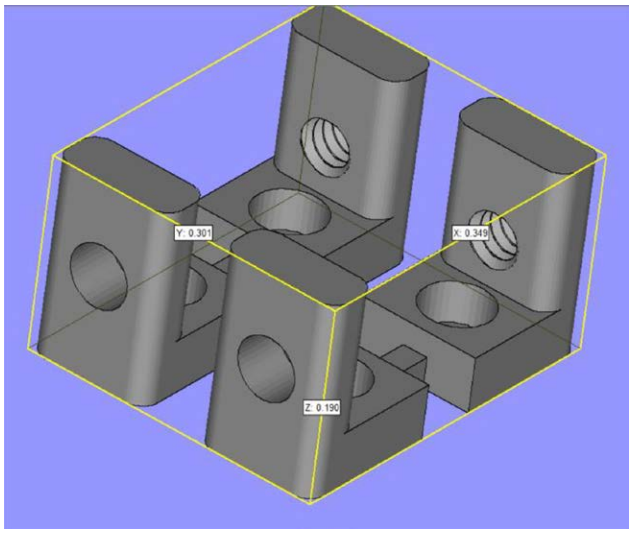

Fig. 1. Development of a lightweight distractor using computer-aided design and 3D printing. Oblique view of tibial distractor plates with length (x), width (y), and height (z) of distractor plate computer-aided design measured in inches.

ketamine hydrochloride (100 mg/kg) and xylazine (5 mg/kg) and subcutaneous yohimbine (1 mg/kg). The surgical site was then prepared. The lower limb was then externally rotated and an incision was made using a 15 blade from the knee to the ankle (Fig. 2A). This leads to exposure of the tibialis anterior, which was divided to expose the tibia (Fig. 2B). Using the handheld dental drill, a 0.6-mm drill bit was then used to drill two holes under continuous saline irrigation—the first, just distal to the tibial tuberosity and the second, along the tibial shaft (Fig. 2C). Each distractor plate was then fixed to the bone using the screws described above (Fig. 2D–F). A transverse osteotomy was then created using a diamond disc saw loaded on a dental saw at the level of the tibial crest under saline irrigation (Fig. 2G, H). The distractor plates were then fixed together using the distractor screw to form a stable unit with the fracture reduced and in acceptable alignment. The muscle was then reapproximated using a 5-0 Vicryl suture, and the skin incision was closed using 5-0 nylon (Fig. 2I).

Tibial Distraction Protocol

The gradual-distraction protocol consisted of a 5-day latency period after the initial osteotomy and fixation of the distraction device, followed by 10 days of distraction at a rate of 0.15 mm every 12 hours (for a total of 3.0 mm) and then 28 days of consolidation. This protocol was developed taking into consideration previously published data on mandible distraction and long bone fracture healing. We previously reported that mandible distraction was successfully completed using this protocol: 5-day latency period after the initial osteotomy and fixation of the distraction device, followed by 10 days of distraction at a rate of 0.15 mm every 12 hours (for a total of 3.0 mm) and then 28 days of consolidation.[31] In addition, our studies on long

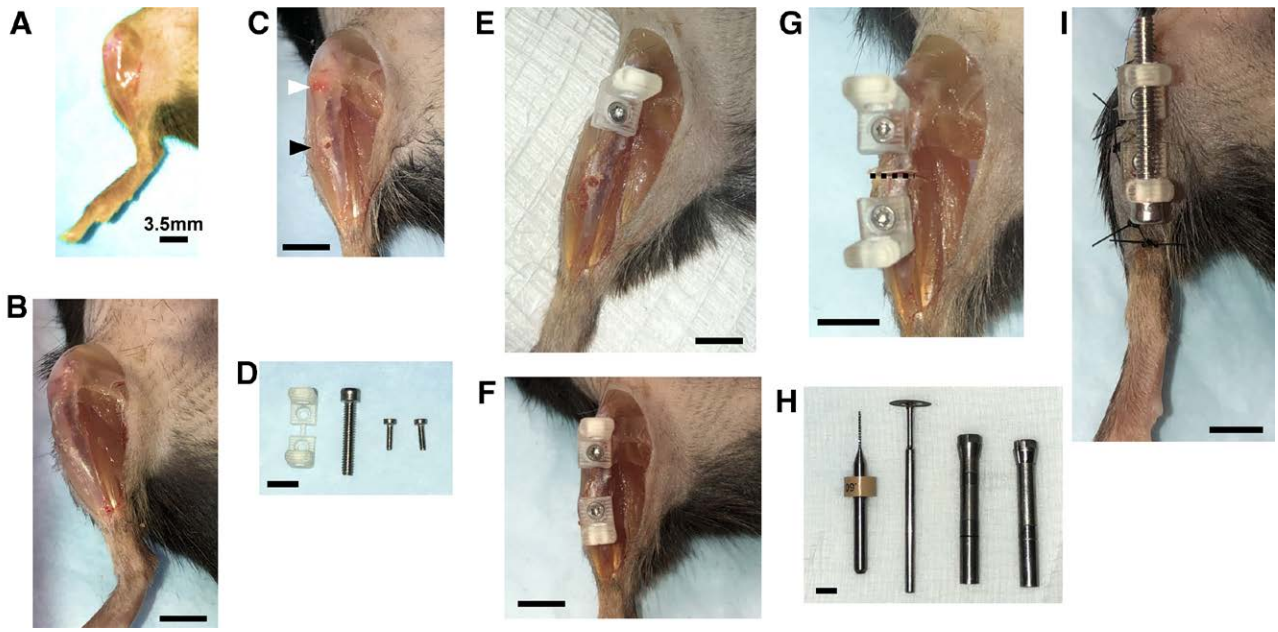

Fig. 2. Tibial distractor placement—surgical technique. A, Preparation of surgical site (shaving and aseptic preparation) followed by lower limb external rotation with incision made from knee to ankle. B, Dissection of tibialis anterior muscle. C, Drill hole at tibial crest shown with white arrowhead, and drill hole at the mid-shaft shown with black arrowhead. D, Left to right: Distractor, distraction screw, and tibial fixation screws. E, Proximal distractor plate shown in situ. F, Distal distractor plate shown in situ. G, Transverse tibial osteotomy creation (broken black line). H, Dental drill equipment: (left to right) 0.6-mm drill bit, Medium MiniFlex Double-Sided Diamond Disc, 3.175-mm chuck (CHK-3.175 91593, Nakanishi Inc., Tokyo, Japan), and 2.35-mm chuck (H203A180A, Brasseler Dental Instrumentation, Ga.). I, Distractor screw in situ with fracture reduction, adequate alignment, and subsequent skin closure. Scale bar on all panels represents 3.5 mm.

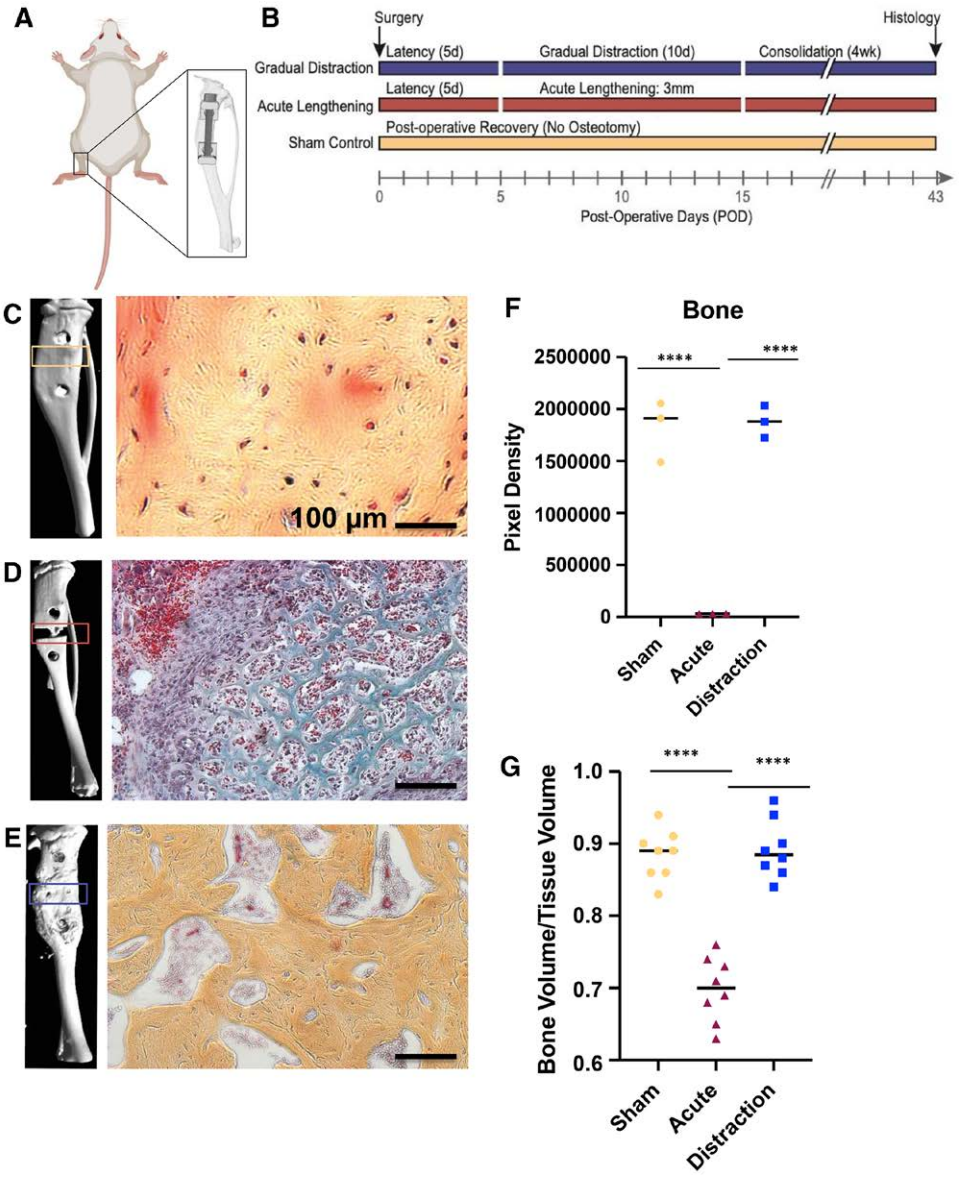

Fig. 3. Tibial distractor—osteogenic validation. A, Mouse tibial distractor schematic. B, Schematic describing protocol timeline for (top to bottom) gradual distraction, acute lengthening, and sham control. The final time point was 43 days postoperatively for all cohorts. C, Left to right: Representative µCT and pentachrome stained section of the sham tibia at POD 43. On pentachrome staining, bone appears yellow, cartilage appears blue-green, muscles appear bright red, and stroma appears brown. Scale bar for all histology images represents 100 µm. D, Left to right: Representative µCT and pentachrome stained section of the acute lengthened tibia at POD 43. E, Left to right: Representative µCT and pentachrome stained section of the gradually distracted tibia at POD 43. F, Graph demonstrating the pixel density of bone following histomorphometric analysis of micrographs of sections obtained from (left to right) sham, acute lengthening, and distraction, which were stained using Movat's pentachrome. G, Graph demonstrating the percentage of bone volume/tissue volume for (left to right) sham, acute lengthening, and distraction, which was analyzed using µCT.

bone fracture healing revealed fracture remodeling by 28 days postoperatively,[34–36] and thus, 28 days of consolidation was hypothesized to be enough time for consolidation to occur. This protocol time course is also similar to those reported in the literature.[32,33]

For the acute-lengthening protocol, lengthening was performed acutely equal to the total distraction amount [3.0-mm acute distraction in one setting, in comparison to the 10 days of distraction at a rate of 0.15 mm every 12 hours (for a total of 3.0 mm) as occurred in the gradual-distraction arm] following a 5-day latency period, with a consolidation period ending at POD 43.

The sham animals underwent preparation, incision, muscle division, and screw drill hole creation without

osteotomy or distractor placement. All specimens from all cohorts were observed daily for postoperative complications and collected at POD 43 (Fig. 3A, B). A total of 11 mice were examined in each cohort.

Micro-computed Tomography

At POD 43, devices were removed before fixation in 2% paraformaldehyde at 4 °C. The tibiae were then scanned using the Bruker Skyscan 1276 with a source voltage of 85 kV, a source current of 200 µA, a filter setting of AI 1 mm, and pixel size of 12 µm at 2016×1344. Phantom targets provided by the manufacturer were used to calibrate instrument measurements. Reconstruction was performed using the NRecon software (Bruker, Mass.), and 3D images were produced using CTVol (Bruker, Mass.). CT histomorphometry was measured using a standardized region of interest of 10 mm as created in DataViewer (Bruker, Mass.) using the CTAn software (Bruker, Mass.). Results were reported in terms of mineralized volume fraction, which is defined as bone volume divided by total tissue volume. A total of eight of the 11 mice were examined in each cohort via micro-computed tomography.

Histology Preparation

Whole tibial tissue specimens were microdissected and kept on ice. Dissected tissue samples were fixed in 2% paraformaldehyde (PFA) at 4 °C overnight and washed with phosphate-buffered saline (PBS) the following day. The specimens were decalcified in 19% EDTA in PBS at 4 °C for 4 weeks with a change of EDTA every 48 hours. Specimens were dehydrated and embedded in paraffin and sectioned at 8 mm. Representative sections were stained with Movat's modified pentachrome solution, which distinguishes the tissues as follows: bone appears yellow, cartilage appears blue-green, muscles appear bright red, and stroma appears brown. A total of three microdissected whole tibiae in each cohort of 11 mice were prepared for histological examination. The samples were quantified for bone composition in pixels using the color deconvolution plug-in on the ImageJ software (National Institutes of Health, Md.).[10,11,37,38]

Statistical Analysis

Statistical analysis was performed using Graph Pad Prism (Calif.). A one-way ANOVA with multiple comparisons was performed for the histological analysis. Unpaired *t* tests were performed for the radiological analyses. Results are shown in brackets as mean ± SD unless otherwise stated.

RESULTS

The Novel, Inexpensive Model of Mouse Tibial Distraction Results in Reproducible Histological and Radiological Bone Regeneration

Implementation of the novel mouse tibial distractor was well tolerated by the mice. Once the mice reached 12 hours postoperatively, all mice were ambulatory. Mouse ambulation was conserved during latency, distraction, and consolidation and in the sham and acute-lengthening subgroups. We did not observe any postoperative complications. Total cost of the distractor and screws used for the model was approximately $11 ($10 per monolateral distractor, <$1 for screws).

Table 1. Summary of All µCT and Histology Results

Condition	Average Mineralized Bone Volume Fraction (Bone Vol/Total Tissue Vol)	Standard Deviation (Bone Vol/Total Tissue Vol)	Bone Proportion as Analyzed on Histology (Pixels)	Standard Deviation (Pixels)
Gradual distraction	0.89	0.04	1,879,257	155,415
Sham	0.89	0.03	1,818,380	293,740
Acute lengthening	0.7	0.04	32,847	1589

Micro-computed Tomography

Micro-computed tomography (µCT) indicated that gradual tibial distraction with the novel device demonstrated increased bone formation relative to acute distraction. The mineralized volume fraction (bone volume/total tissue volume) of the bone regenerate was significantly increased in gradual distraction (mean, 0.9±0.1) compared to the acute-lengthening group (mean, 0.7±0.1; $P < 0.001$) (Fig. 3C–E, G; Table 1). There was no significant difference in the mineralized volume fraction between the gradual distraction and sham ($P = 0.69$). The percent difference between gradual distraction and acute lengthening was 21.6% ± 6.1%, and the difference between gradual distraction and sham was 4.0% ± 3.1% (Table 2).

Histology

Pentachrome staining indicated that gradual tibial distraction with the novel device demonstrated bone formation (Fig. 3C–F). The proportion of bone in the specimen was significantly greater in the gradual-distraction group (1,879,257±155,415 pixels) in comparison to acute lengthening (32,847±15,89 pixels) ($P < 0.0001$), but there was no significant difference in the proportion of bone in the distraction group relative to the sham group ($P = 0.69$) (Fig. 3C–F; Table 1). The percent difference between gradual distraction and acute lengthening was 98.2% ± 0.2%, while the percent difference between gradual distraction and sham was 5.4% ± 7.1% (Table 2). The acute lengthened tibias resulted in nonunion with minimal bone presence histologically (Fig. 3D, F). Sham (uninjured) tibias had normal bone morphology at POD 43 (Fig. 3C, F). A complete summary of all µCT and histology results is reported in Table 1, and a summary of all relevant percent differences and *P* values is reported in Table 2.

DISCUSSION

Following the implementation of a computer-aided design, together with commercially available screws, we demonstrate a novel mouse model of tibial DO, which

Table 2. Summary of Percent Differences and *P* Values between Gradual Distraction and Sham or Acute Distraction Conditions

Conditions Compared	Percent Difference of Average Mineralized Bone Volume Fraction (%)	Standard Deviation (%)	*P*	Percent Difference of Bone Proportion (%)	Standard Deviation (%)	*P*
Sham compared with gradual distraction	3.95	3.06	0.69	5.42	7.08	0.69
Acute lengthening compared with gradual distraction	21.58	6.05	<0.001	98.24	0.20	<0.0001

results in bone regeneration, which is demonstrated histologically and using μCT. We validated these results against sham surgery and acute lengthening. Acute lengthening demonstrated features consistent with a fibrous union, such as low-average mineralized bone volume fraction on μCT (0.7±0.1) compared with the gradual DO group (0.9±0.1), and the presence of cartilage on histology (blue area on Movat's modified pentachrome). A fibrous union after acute lengthening is demonstrated in prior animal studies.[5,31] For example, a higher percentage of stroma and cartilage was seen on pentachrome staining of the bone regenerate when comparing mandibles that underwent acute lengthening compared to those that underwent gradual distraction.[31]

In comparison with existing mouse tibial DO literature, our model is unique in the type of distractor used. Many of the other models use a circular frame distractor that may limit mobility[25–27,39,40] or a monolateral frame that is less bulky but may require more invasive surgery to secure the distractor around the tibial bone.[29,30] While the other studies do not state the cost of their devices for DO, our distractor is relatively low cost ($10 per monolateral distractor, <$1 for screws) and lightweight, composed of lightweight UV-cured photopolymer. In comparison, other mouse studies use a number of materials that were either adapted from specialized dental equipment or human craniofacial DO,[25,26,30] and many used materials, such as immediate polymerization resin,[25] stainless steel,[30] or aluminum[27] frames. These materials are more costly than our distractor. Our model also uses 3D printing to create the distractor, which makes it accessible to anyone with 3D printing capabilities. Advantages of 3D printing are rapid production, a low amount of production steps, and easy adaptability,[41] in contrast to other distractors that may use multiple molding steps to produce the final product.[25] It is difficult to directly compare results of various studies because the distractor used, distraction distance, and length of time of the latency, distraction, and consolidation phases are different in each study.[25–30,40,42] The results of our distraction model consistently demonstrated osteogenesis with no fibrous union seen at the final time point (POD 43). If the distractor results in relative stability post-osteotomy, one should see evidence of fibrous nonunion or malunion, as is seen clinically.[7] Furthermore, our model was not associated with complications. Other models report complications, such as unstable fixation and loss of alignment[26,30] as well as necrosis distal to the distractor[26]; therefore, our model provides the benefit of a relatively low complication rate.

The limitations of this study include that although we observed grossly that mice were weight-bearing on POD 0, we did not do a detailed analysis on the impact of the distractor on mouse mobility. We also only studied male mice. While there are currently no experimental studies of sex differences in mouse DO and there is generally inconclusive evidence on fracture healing in men versus women,[42,43] sex can indeed affect osteogenesis and remodeling. Increased weight and, therefore, mechanical loading in male mice, as well as increased β-catenin/Wnt signaling was shown to improve fracture healing in a rigid fixation mouse model,[44] and the implications of such findings on DO should be evaluated in future studies. In addition, while our distractor is rigid along the axis of the distractor screw, great care must be taken during the process of distraction to prevent rotation of the bone ends around this axis. Since DO is predicated on the idea that holding the two bone ends in tension allows for parallel column growth of new bone,[5] a disruption of this parallel collagen scaffolding may lead to disruption of the bone regeneration process. Finally, we did not perform a power calculation.

In conclusion, herein we describe a preliminary model of mouse tibial distraction, which can be further implemented in genetically dissectible mouse models, allowing us to better understand the genetic basis and pathophysiology of this powerful regenerative technique in mice. We demonstrate the development of a mouse model of tibial DO, which utilizes computer-aided design of a lightweight monolateral fixator in addition to commercially available screws.

Michael T. Longaker, MD, MBA, FACS
Hagey Laboratory for Pediatric Regenerative Medicine
Department of Surgery
Stanford University School of Medicine
257 Campus Drive
Stanford, CA 94305-5418
E-mail: longaker@stanford.edu

Derrick C. Wan, MD
Hagey Laboratory for Pediatric Regenerative Medicine
Department of Surgery
Stanford University School of Medicine
257 Campus Drive
Stanford, CA 94305-5418
E-mail: dwan@stanford.edu

REFERENCES

1. Keating JF, Simpson AH, Robinson CM. The management of fractures with bone loss. *J Bone Joint Surg Br.* 2005;87:142–150.
2. Houben RH, Thaler R, Kotsougiani D, et al. Neo-angiogenesis, transplant viability, and molecular analyses of vascularized bone

allotransplantation surgery in a large animal model. *J Orthop Res.* 2020;38:288–296.
3. Houben RH, Kotsougiani D, Friedrich PF, et al. Outcomes of vascularized bone allotransplantation with surgically induced autogenous angiogenesis in a large animal model: bone healing, remodeling, and material properties. *J Reconstr Microsurg.* 2020;36:82–92.
4. Codivilla A. The classic: on the means of lengthening, in the lower limbs, the muscles and tissues which are shortened through deformity [1905]. *Clin Orthop Relat Res.* 2008;466:2903–2909.
5. Ilizarov GA. The tension-stress effect on the genesis and growth of tissues: part II. The influence of the rate and frequency of distraction. *Clin Orthop Relat Res.* 1989;(239):263–285.
6. Ilizarov GA. The tension-stress effect on the genesis and growth of tissues. Part I. The influence of stability of fixation and soft-tissue preservation. *Clin Orthop Relat Res.* 1989;(238):249–281.
7. Lowenberg DW, Randall RL. The Ilizarov method. *Surg Technol Int.* 1993;2:459–462.
8. Hosny GA. Limb lengthening history, evolution, complications and current concepts. *J Orthop Traumatol.* 2020;21:3.
9. Liantis P, Mavrogenis AF, Stavropoulos NA, et al. Risk factors for and complications of distraction osteogenesis. *Eur J Orthop Surg Traumatol.* 2014;24:693–698.
10. Kumabe Y, Fukui T, Takahara S, et al. Percutaneous CO2 treatment accelerates bone generation during distraction osteogenesis in rabbits. *Clin Orthop Relat Res.* 2020;478:1922–1935.
11. Li Y, Li R, Hu J, et al. Recombinant human bone morphogenetic protein-2 suspended in fibrin glue enhances bone formation during distraction osteogenesis in rabbits. *Arch Med Sci.* 2016;12:494–501.
12. Al-Sebaei MO, Gagari E, Papageorge M. Mandibular distraction osteogenesis: a rabbit model using a novel experimental design. *J Oral Maxillofac Surg.* 2005;63:664–672.
13. Bail HJ, Raschke MJ, Kolbeck S, et al. Recombinant species-specific growth hormone increases hard callus formation in distraction osteogenesis. *Bone.* 2002;30:117–124.
14. Bail HJ, Kolbeck S, Krummrey G, et al. Ultrasound can predict regenerate stiffness in distraction osteogenesis. *Clin Orthop Relat Res.* 2002;404:362–367.
15. Raschke MJ, Bail H, Windhagen HJ, et al. Recombinant growth hormone accelerates bone regenerate consolidation in distraction osteogenesis. *Bone.* 1999;24:81–88.
16. Lewis DD, Kim SE, Shmalberg J, et al. Correction of excessive tibial plateau angle and limb shortening in a juvenile dog using a hinged circular fixator construct and distraction osteogenesis. *Case Rep Vet Med.* 2019;2019:1439237.
17. Klotch DW, Ganey TM, Slater-Haase A, et al. Assessment of bone formation during osteoneogenesis: a canine model. *Otolaryngol Head Neck Surg.* 1995;112:291–302.
18. Shen J, Sun Y, Liu X, et al. EGFL6 regulates angiogenesis and osteogenesis in distraction osteogenesis via Wnt/β-catenin signaling. *Stem Cell Res Ther.* 2021;12:415.
19. Wang F, Kong L, Wang W, et al. Adrenomedullin 2 improves bone regeneration in type 1 diabetic rats by restoring imbalanced macrophage polarization and impaired osteogenesis. *Stem Cell Res Ther.* 2021;12:288.
20. Roseren F, Pithioux M, Robert S, et al. Systemic administration of G-CSF accelerates bone regeneration and modulates mobilization of progenitor cells in a rat model of distraction osteogenesis. *Int J Mol Sci.* 2021;22:3505.
21. Aronson J, Hogue WR, Flahiff CM, et al. Development of tensile strength during distraction osteogenesis in a rat model. *J Orthop Res.* 2001;19:64–69.
22. McDonald MM, Morse A, Birke O, et al. Sclerostin antibody enhances bone formation in a rat model of distraction osteogenesis. *J Orthop Res.* 2018;36:1106–1113.
23. Jazrawi LM, Majeska RJ, Klein ML, et al. Bone and cartilage formation in an experimental model of distraction osteogenesis. *J Orthop Trauma.* 1998;12:111–116.
24. Matsuno M, Hata K, Sumi Y, et al. In vitro analysis of distraction osteogenesis. *J Craniofac Surg.* 2000;11:303–307.
25. Fujio M, Osawa Y, Matsushita M, et al. A mouse distraction osteogenesis model. *J Vis Exp.* 2018;141.
26. Tay BK, Le AX, Gould SE, et al. Histochemical and molecular analyses of distraction osteogenesis in a mouse model. *J Orthop Res.* 1998;16:636–642.
27. Yukata K, Nikawa T, Takahashi M, et al. Overexpressed osteoactivin reduced osteoclastic callus resorption during distraction osteogenesis in mice. *J Pediatr Orthop B.* 2021;30:500–506.
28. Fowlkes JL, Nyman JS, Bunn RC, et al. Osteo-promoting effects of insulin-like growth factor I (IGF-I) in a mouse model of type 1 diabetes. *Bone.* 2013;57:36–40.
29. Jacobsen KA, Al-Aql ZS, Wan C, et al. Bone formation during distraction osteogenesis is dependent on both VEGFR1 and VEGFR2 signaling. *J Bone Miner Res.* 2008;23:596–609.
30. Carvalho RS, Einhorn TA, Lehmann W, et al. The role of angiogenesis in a murine tibial model of distraction osteogenesis. *Bone.* 2004;34:849–861.
31. Ransom RC, Carter AC, Salhotra A, et al. Mechanoresponsive stem cells acquire neural crest fate in jaw regeneration. *Nature.* 2018;563:514–521.
32. Kasaai B, Moffatt P, Al-Salmi L, et al. Spatial and temporal localization of WNT signaling proteins in a mouse model of distraction osteogenesis. *J Histochem Cytochem.* 2012;60:219–228.
33. Zhang N, Hua Y, Li Y, et al. Sema3A accelerates bone formation during distraction osteogenesis in mice. *Connect Tissue Res.* 2021;63:382–392.
34. Murphy MP, Koepke LS, Lopez MT, et al. Articular cartilage regeneration by activated skeletal stem cells. *Nat Med.* 2020;26:1583–1592.
35. Tevlin R, Seo EY, Marecic O, et al. Pharmacological rescue of diabetic skeletal stem cell niches. *Sci Transl Med.* 2017;9:eaag2809.
36. Marecic O, Tevlin R, McArdle A, et al. Identification and characterization of an injury-induced skeletal progenitor. *Proc Natl Acad Sci USA.* 2015;112:9920–9925.
37. Kim JB, Lee DY, Seo SG, et al. Demineralized bone matrix injection in consolidation phase enhances bone regeneration in distraction osteogenesis via endochondral bone formation. *Clin Orthop Surg.* 2015;7:383–391.
38. Singh S, Song HR, Venkatesh KP, et al. Analysis of callus pattern of tibia lengthening in achondroplasia and a novel method of regeneration assessment using pixel values. *Skeletal Radiol.* 2010;39:261–266.
39. Haque T, Hamade F, Alam N, et al. Characterizing the BMP pathway in a wild type mouse model of distraction osteogenesis. *Bone.* 2008;42:1144–1153.
40. Isefuku S, Joyner CJ, Reed AAC, et al. Distraction osteogenesis in the Cbfa-1± mouse. *J of Orthop Res.* 2004;22:1276–1282.
41. Gibson I, Rosen D, Stucker B. Additive manufacturing technologies: 3D printing, rapid prototyping, and direct digital manufacturing. *Springer Publ Company.* 2015;2:9–10.
42. Collier CD, Hausman BS, Zulqadar SH, et al. Characterization of a reproducible model of fracture healing in mice using an open femoral osteotomy. *Bone Rep.* 2020;12:100250.
43. Working ZM, Morris ER, Chang JC, et al. A quantitative serum biomarker of circulating collagen X effectively correlates with endochondral fracture healing. *J Orthop Res.* 2021;39:53–62.
44. Haffner-Luntzer M, Fischer V, Ignatius A. Differences in fracture healing between female and male C57BL/6J mice. *Front Physiol.* 2021;12:712494.